Wheel arches and ground clearance sizing of Fiat Uno 1.0L 1989

Master's Degree in Automotive Engineering

Loris Fonseca: s342696@studenti.polito.it

Nikoloz Kapanadze: s342649@studenti.polito.it

Maurizio Pio Vergara: s346643@studenti.polito.it

Renis Shtylla: s344685@studenti.polito.it

a.a 2024/2025

Contents

1 Introduction

The definition of the wheel arches profile is of fundamental importance when designing the body profile of the vehicle. A good wheel arch must provide the correct functioning of steering system, must avoid interference between tyre and car body and has to be compliant with suspensions travel. To accomplish these requirements, the following parameters must be taken into account: steering angle during kinematic steering, steering axis, suspensions displacement and size of wheels, including extra space for dirt and chains. Moreover, the integration with other vehicle subsystems must be carefully considered to prevent any potential interference with the wheel arch.

The first step to perform this analysis is to select a commercial vehicle and extract the required data, which are: wheelbase, track, size of tires, minimum steering radius, number of occupants, position of the occupants in side view, mass and weight distribution in empty load. In Table 1 the data relative to Fiat Uno 1.0L 1989 are reported.

l	2362	mm	Wheelbase
L	3689	mm	Length
w	1558	mm	Width
C_f	1343	mm	Front track
C_r	1300	mm	Rear track
m	805	kg	Mass Curb weight
m_d	770	kg	Mass Dry weight
R	4700	mm	Curb to curb radius
135/80 R13		Maximum tyre label	
65% front - 35 %rear		Weight distribution	

Table 1: Fiat Uno 1.0L 1989 data

2 Maximum tire size

The first parameter that has to be evaluated in order to properly design the wheel arch profile is the maximum tire size that can be mounted on the vehicle. Specifically, for the vehicle analyzed in this study, the 1989 Fiat Uno 1.0, the largest compatible tire size is labeled as 135/80 R13, as shown in Table 1. Hence, the maximum wheel diameter can be easily estimated according to the following formula:

$$D_{max} = 13 \cdot 25.4 + 2 \cdot \frac{80}{100} \cdot 135 = 546.2\,\text{mm}$$

Moreover, tyre maximum width, directly reported on the tyre labeling as first number, is:

$$w_{tire,max} = 135\,\text{mm}$$

The sketch of the tire corresponding to the maximum wheel dimensions is depicted in Figure 1.

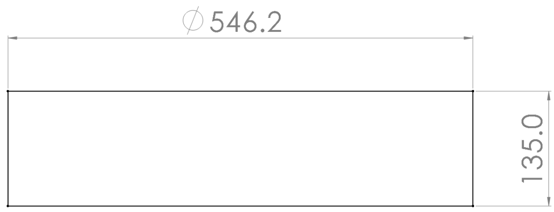

Figure 1: Tire's maximum dimensions

3 Wheel arches sizing

The wheel arch profile can be designed through two types of analyses: a top-view design and a side-view design. A qualitative representation of the wheel arch profile in top view is depicted in Figure 2, along with other vehicle subsystems such as the gearbox (GB), steering rack (SR), tunnel (T), firewall (FW), trimmings (TR) and pedals (P).

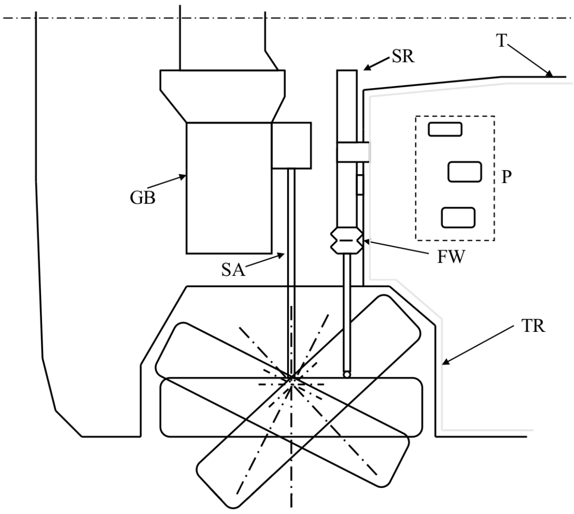

Figure 2: Wheel arch profile and related vehicle subsystems

4 Top view wheel arch design

The analyzed vehicle, the Fiat Uno, is characterized by front-wheel steering, thus two distinct wheel arches are designed: one for the front, considering the steering angles of the wheels, and one for the rear, considering a fixed angular position of the tires. Moreover, since snow chains can only be mounted on the front wheels, their size will be taken into account exclusively in the assessment of the front wheel arch. Finally, an extra margin is considered to guarantee proper and safe functionality even when the gap between the tire and the wheel arch is diminished due to the accumulation of dirt and snow.

Both the front and rear analyses are carried out considering the maximum tire dimensions, evaluated in Section 2 and illustrated in Figure 1.

4.1 Maximum steering angle evaluation

The first step to be performed for the evaluation of the top view wheel arch profile is the definition of tyre's maximum steering angles, indicated with δ_1 and δ_2 in Figure 3. These angles are of fundamental importance when designing the front wheel arch since a proper clearance between the tire and the wheel arch must be ensured for whatever steering angle.

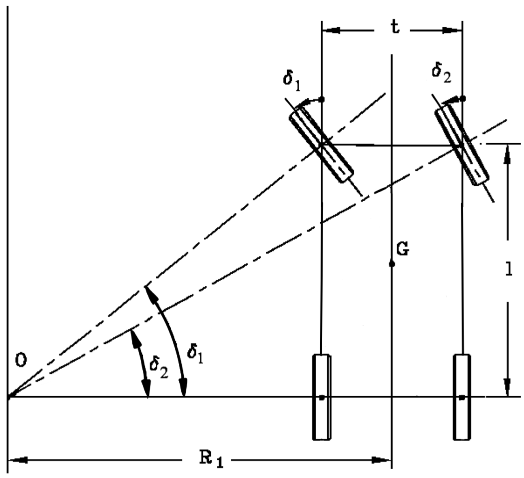

Figure 3: Kinematic steering of a vehicle

The values of these two angles can be evaluated through the following equations:

$$\delta_1 = \arctan\left(\frac{l}{R_1 - \frac{t}{2}}\right) \tag{1}$$

$$\delta_2 = \arctan\left(\frac{l}{R_1 + \frac{t}{2}}\right) \tag{2}$$

$$R_1 = \sqrt{R^2 - l^2} - \frac{t}{2} \tag{3}$$

where l is the wheelbase, R is the minimum steering radius and t is the front track (C_f).

By substituting into Equations 1 and 2 the corresponding data reported in Table 1, the following maximum steering angles are obtained: $\delta_1 = 40.97^\circ$ and $\delta_2 = 30.17^\circ$.

4.2 Front wheel arch design

The front wheel arch must ensure the proper functioning of the steering system by providing sufficient clearance for the tires during kinematic steering. To properly design the front wheel arch, it is essential to account for the two extreme conditions that arise during kinematic steering operation, namely: maximum wheel turn inward and maximum wheel turn outward. This two characteristics are related to the angles evaluated in Section 4.1.

Initially, the profile lines are sketched with the steering angle set to zero. From this initial condition, the tire trajectories are then evaluated by rotating the tire around the steering axis of δ_1 and δ_2. In this survey, the steering axis is positioned at the intersection between the internal edge of the tire and the driveshaft axis. Tire trajectories provide a precise outline of the tire's movement, which is then used as a reference to define the shape of the wheel arch, ensuring that it accommodates the full range of motion of the tire during steering. In Figure 4, the resulting tire trajectories are reported with color red.

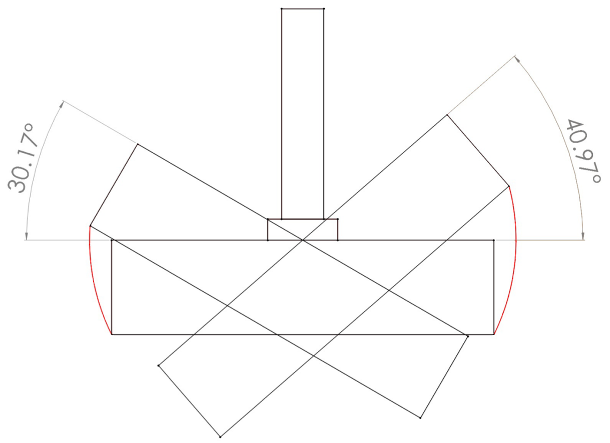

Figure 4: Tire trajectories during kinematic steering

Once the wheel arch shape ha been designed, the last step is the evaluation of the clearance between the tire and the wheel arch. As previously mentioned, it is defined starting from the envelope of the maximum tire dimensions. To this, an additional margin is added to account for the dimensions of snow chains, the thickness of dirt or snow layers, and a safety allowance for safety considerations. According to the user manual of the Fiat Uno, the maximum dimension for snow chains is limited to 12 mm. Furthermore, a layer of dirt and snow measuring 15 mm and a safety margin of 25 mm are considered. Hence, the total offset between the tire of maximum dimensions and the wheel arch profile in the top view analysis is computed as follows:

$$\text{tire-wheel arch clearance} = 12 + 15 + 25 = 52\,\text{mm}$$

Therefore, having the wheel arch shape and the distance from the tire, the longitudinal wheel arch profile can be sketched, as reported in Figure 5.

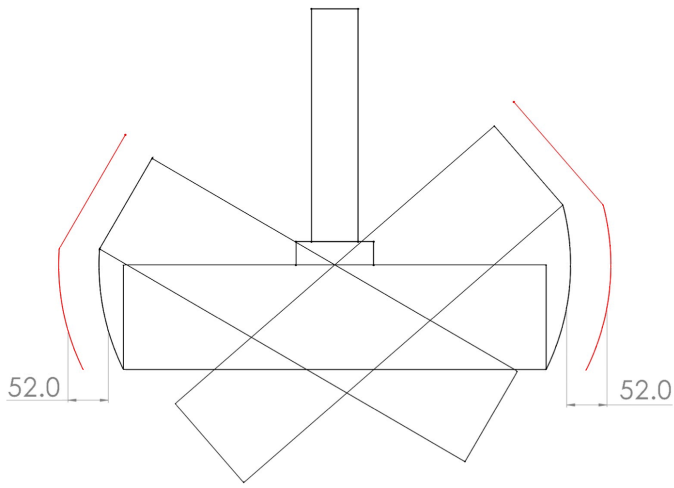

Figure 5: Clearance between the tire trajectory and the wheel arch profile

To complete the top view front wheel arch design, the profile must be closed, ensuring a continuous contour that fully encloses the tire and the suspension within the wheel arch, as shown in Figure 6.

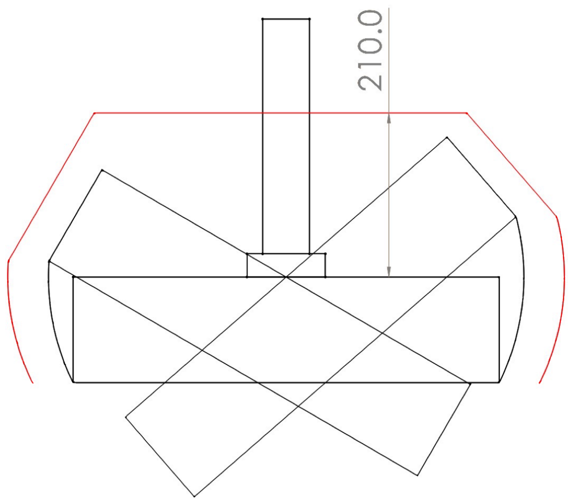

Figure 6: Closed profile of the front wheel arch

The final profile of the front wheel arch in top view is hence obtained and reported in Figure 7.

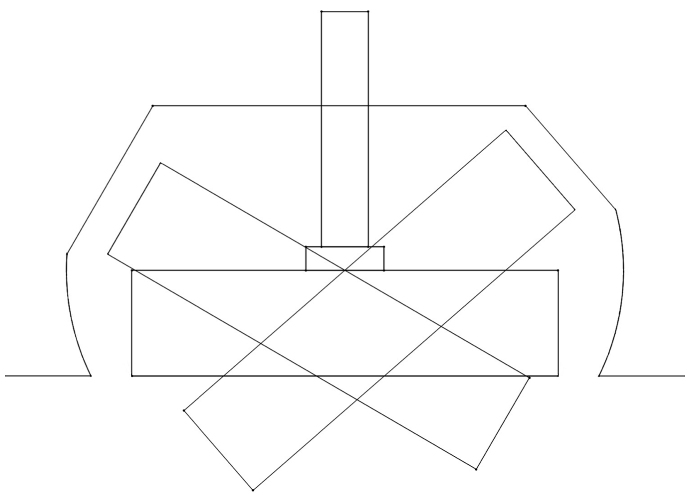

Figure 7: Top view front wheel arch

4.3 Rear wheel arch design

The rear wheel arch design is simpler with respect to the front one since it does not need to account for the rotation of the wheels. The only constraint that must be considered is the suspension bulk. Therefore, the evaluation of the clearance between the tires and the rear wheel arch takes into consideration only the thickness of dirt and snow layer and the safety allowance. Hence, the longitudinal distance between the tire and the wheel arch is evaluate as follow:

$$\text{tire-wheel arch clearance} = 15 + 25 = 40\,\text{mm}$$

As previously mentioned, the thickness of the snow chains is not considered since the analyzed vehicle can only mount them on the front axle. Starting from the tire with maximum dimensions, the longitudinal profile of the wheel arch can be sketched by simply considering parallel lines with the tire's envelope, as depicted in Figure 8.

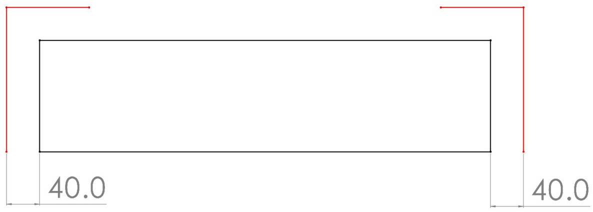

Figure 8: Clearance between the rear tire and the wheel arch profile

The final contour of the rear wheel arch is determined by incorporating a slot to accommodate the suspension housing. The resulting profile is illustrated in Figure 9.

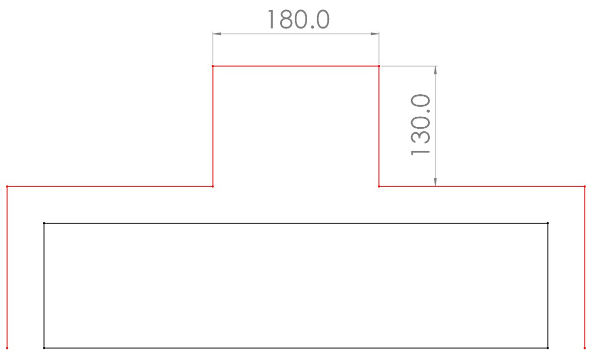

Figure 9: Closed profile of the rear wheel arch

The final profile of the rear wheel arch in top view is hence obtained and reported in Figure 10.

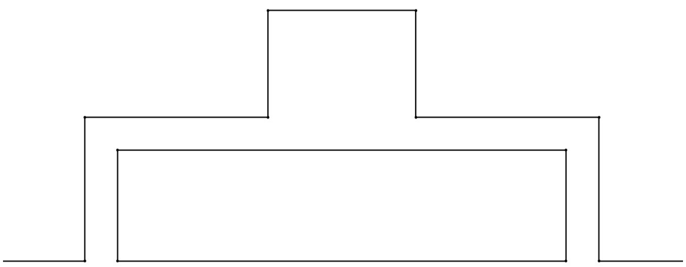

Figure 10: Top view rear wheel arch

5 Top view sketch of Fiat Uno

In this section a qualitative sketch, in top view, of the Fiat Uno is reported. The vehicle's profile is outlined based on the assessed wheel arch contours, along with different vehicle subsystems.

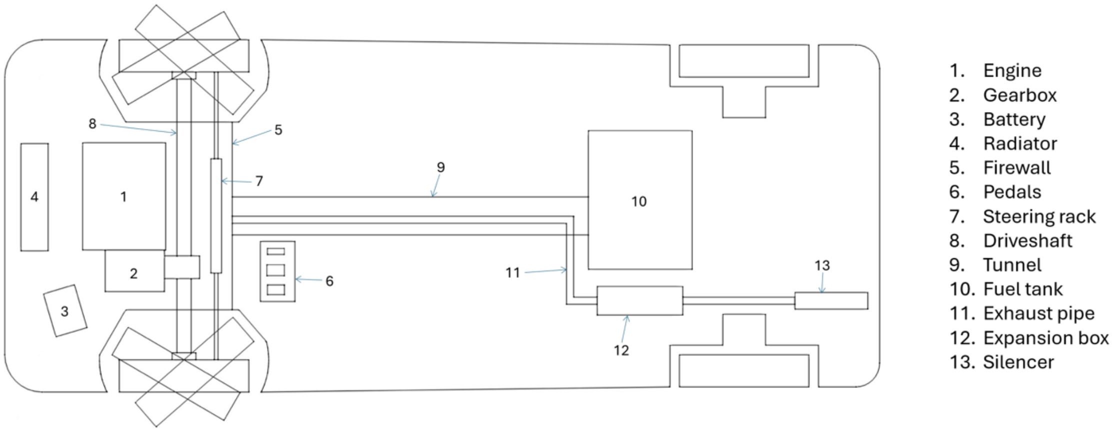

Figure 11: Top view schematic of the Fiat Uno layout with key components

6 Side view wheel arch design

The evaluation of the side view wheel arch profile is carried out by taking into consideration the movement of the suspensions. This approach ensures that the profile accommodates the dynamic behavior of the suspension system, allowing for adequate clearance during compression and rebound phases, and avoiding potential interference between the wheel and the bodywork, even when the suspension reaches its maximum travel.

6.1 Load distribution evaluation

To accurately evaluate the suspension travel, different loading conditions are analyzed and reported as follows:

- Standard A: curb weight
- Standard B: A + 70kg front passenger + 10kg luggage
- Standard C: B + 70kg front passenger + 10kg luggage
- Standard D: C + 70kg rear passenger + 10kg luggage
- Standard E: D + 70kg rear passenger + 10kg luggage
- Standard F: E + 70kg rear passenger + 10kg luggage

The loads associated with the front passengers, rear passengers, and luggage are illustrated in Figure 12, along with their relative distances from the front or rear axle. In particular:

- F_F: Front axle load
- F_R: Real axle load
- F_{PF}: Front Passengers load
- F_{PR}: Rear Passengers load
- F_L: Luggage load
- a = 826.7 mm: distance between front axle and curb vehicle centre of gravity
- b = 1535.3 mm: distance between rear axle and curb vehicle centre of gravity
- c = 1189.0 mm: distance between front axle and front passenger load
- d = 319.6 mm: distance between rear axle and rear passenger load
- e = 252.4 mm: distance between rear axle and luggage load

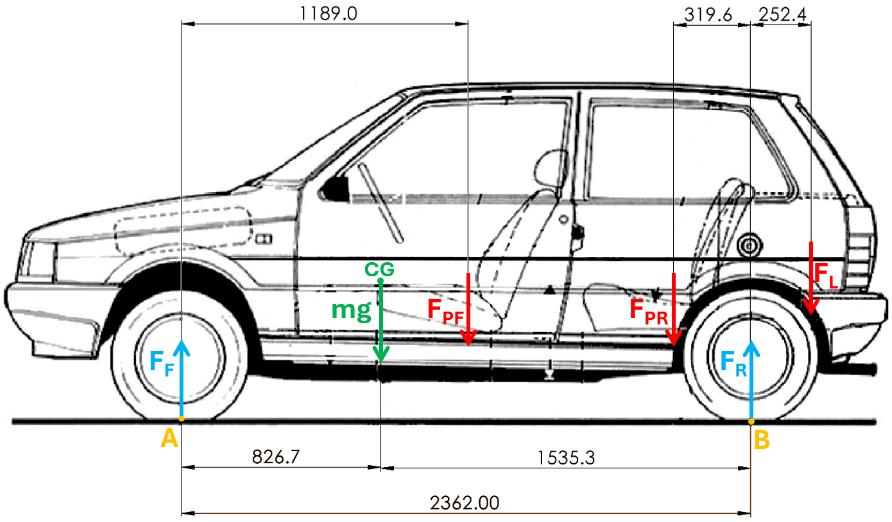

Figure 12: Vehicle applied loads and relative position

The values of c, d and e are extracted from the vehicle geometry, while a and b are evaluated starting from the weight distribution and the wheelbase as follows:

$$a = 0.35 \cdot w_b \tag{4}$$

$$b = 0.65 \cdot w_b \tag{5}$$

The calculation of the front and rear axle forces is performed by exploiting the moment equilibrium equation about point A and B. The resulting formulas evaluated through this procedure are reported in Equation 6 and 7.

$$F_F = \frac{F_{PR} \cdot d + F_{PF}(w_b - c) - F_L \cdot e + mg \cdot b}{w_b} \tag{6}$$

$$F_R = \frac{F_{PR}(w_b - d) + F_{PF} \cdot c + F_L(w_b + e) + mg \cdot a}{w_b} \tag{7}$$

The values of front and rear axle force forces, evaluated according to the standards defined above, are reported in Table 2.

Standard	Front axle force F_F [N]	Rear axle force F_R [N]
A	5133.1	2764.0
B	5463.6	3218.2
C	5794.2	3672.5
D	5876.6	4374.9
E	5959.0	5077.2
F	6041.5	5779.6

Table 2: Front and Rear axle forces relative to the standard loadcases

Starting from the axle forces, it is also possible to evaluate the load distribution in the different loading conditions. The results are reported in Table 3.

Standard	Load distribution: Front - Rear [%]
A	65-35
B	63-37
C	61-39
D	57-43
E	54-46
F	51-49

Table 3: Load distribution relative to the standard loadcases

It can be observed that Standard A has the highest front-heavy distribution, with 65% of the weight at the front and 35% at the rear. As we move down the list, the front weight percentage decreases, with Standard F exhibiting the most balanced distribution, with a 51-49% split between the front and rear. The amount of load distribution can lead to different advantages and drawbacks: a front-heavy distribution can provide better traction on the front tires, especially in conditions where grip is important (e.g. on slippery roads or when accelerating). Moreover, with more weight over the front, braking efficiency may be improved, as the front tires bear more of the braking load. On the other hand, a more balanced load distribution typically improves the vehicle's handling during cornering. It allows for more effective weight transfer, helping to reduce understeering or oversteering. Additionally, with a more balanced weight distribution, tire wear may be more evenly distributed across the front and rear tires, leading to longer tire life.

6.2 Suspension stiffness evaluation

The stiffness evaluation is of fundamental importance for the computation of the suspensions travel under the different loading conditions. Indeed, it directly determines how the suspension responds when subjected to external loads.

Since no information about the stiffness values of front and rear suspensions is available, an alternative approach must be must be adopted to determine them. This approach is based on some considerations about the suspensions resonance frequency that are taken into account during the design phase of this subsystem.

The analysis of the suspension motions of a vehicle is usually conducted using the so-called quarter car model, depicted in Figure 13. This model considers a single wheel with its related suspension and the portion of the vehicle body supported by that wheel. The tire is considered as a massless spring, connected in parallel with a shock absorber to the unsprung mass. The body weight of the vehicle is considered in the sprung mass, while a spring-damper connection between the two masses models the suspension. Since two masses are present, this model is characterized by two degrees of freedom.

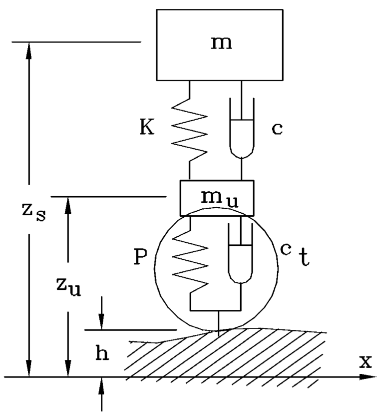

Figure 13: Quarter car model with two degrees of freedom

The model can be modified in order to simplify the analysis. In particular, since the sprung mass is significantly greater than the unsprung mass, the system's frequency response is primarily dominated by the sprung mass. As a result, the unsprung mass can be neglected, as it has minimal impact on passengers comfort, which instead is closely related to the behavior of the sprung mass. Therefore, in the simplified model, the tires are considered as massless rigid bodies, connected to the single sprung mass through a spring-damper connection. Since only one mass is considered, this model is characterized by a single degree of freedom.

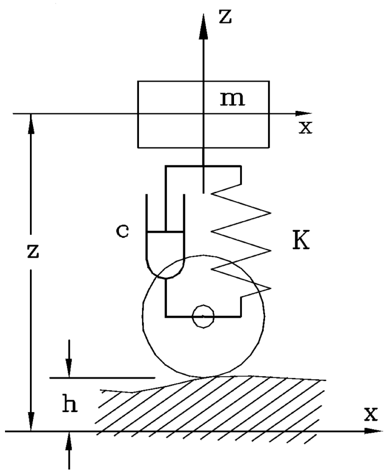

Figure 14: Quarter car model with one degree of freedom

The so obtained model is a simple mass-spring-damper system, which is characterized by a natural frequency evaluated according to Equation 8.

$$f_n = \frac{1}{2\pi} \cdot \sqrt{\frac{k}{m}} \tag{8}$$

The natural frequency represents the specific frequency at which the system's response to an input is highly amplified, as reported in Figure 15. Therefore, the objective in designing the suspension stiffness is to position the natural frequency of the system such that the discomfort perceived by the passengers is minimized, thus keeping f_n away from the frequency ranges most sensitive to humans.

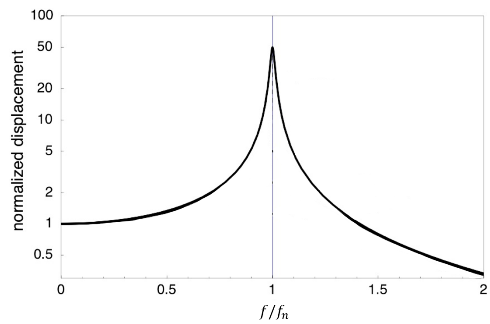

Figure 15: Frequency response of the quarter car model with a single degree of freedom

In Figure 16, the human body sensitivity as function of the frequency is plotted.

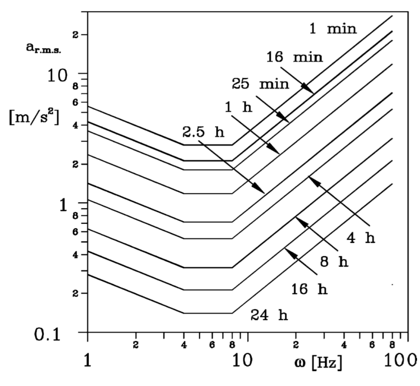

Figure 16: Human body sensitivity to vibrations

It can be noticed that the frequency range in which humans are more affected by vibrations lies between 4 and 8 Hz. Moreover, very low frequencies produce sensations related to motion sickness, while too high frequencies may cause organ injuries. Based on these considerations, the resonance frequency of vehicle suspensions is typically designed to fall within a range around 1.5 Hz.

Therefore, by assuming f_n = 1.5 Hz, the suspension stiffness can be evaluated with the following formula, derived from Equation 8:

$$k = m \cdot (2\pi f_n)^2 \tag{9}$$

Generally, the suspension stiffness is not the same for both the axles, therefore two different stiffness values can be computed, one for the rear axle and one for the front axle. Depending on the analyzed case, the corresponding load on the axle, F_F for the front and F_R for the rear, must be considered. However, in order to exploit the relation shown in Equation 9, the equivalent masses corresponding to front and rear load must be computed. The following simple relation can be employed:

$$m_F = \frac{F_F}{g} \tag{10}$$

$$m_R = \frac{F_R}{g} \tag{11}$$

The force to displacement characteristic of vehicle suspension spring is depicted in Figure 17. The curve exhibits a linear region near the y-axis, meanwhile for larger values of the displacement the curve becames non linear. Under typical operating conditions, the spring primarily functions within the linear region of the curve, entering the nonlinear domain only at extreme displacement values. These extreme conditions may arise, for example, from encountering obstacles or bumps on the road.

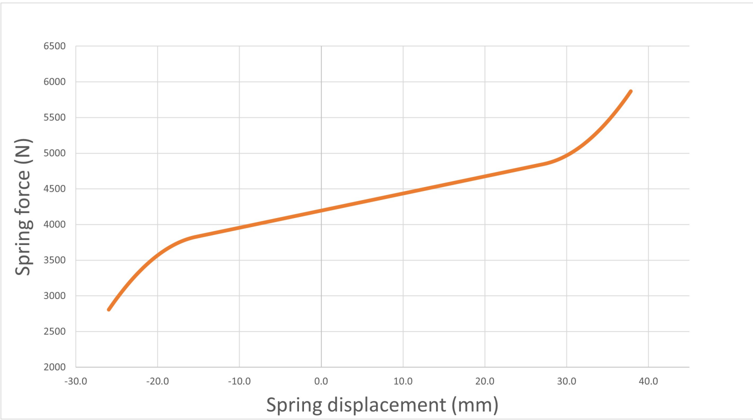

Figure 17: Force-to-displacement characteristic of a vehicle suspension

In this study, only standard operating conditions are considered, ensuring that the spring deflection remains within the linear region. As a result, the stiffness value remains constant. Therefore, a single loading condition is sufficient for evaluating the stiffness values for both the front and rear axle. In this study, the load standard F is considered. Using Equation 10 and 11, the calculated masses of the front and rear sections, under standard F loading condition, are the following:

$$m_F = 615.8 \text{ kg}$$

$$m_R = 589.2 \text{ kg}$$

The stiffness values for the front and rear axles are determined using Equation 9, yielding:

$$k_{FrontAxle} = 54704 \ \frac{N}{m}$$

$$k_{RearAxle} = 52332 \ \frac{N}{m}$$

These stiffness values represent the characteristics of the entire axle. To calculate the stiffness of the individual spring mounted on each tire suspension, the axle stiffness values are divided by two, as expressed by the following equation:

$$k_{Front,RearTire} = \frac{k_{Front,RearAxle}}{2} \tag{12}$$

The resulting stiffness values of the single springs are:

$$k_{FrontTire} = 27352 \ \frac{N}{m}$$

$$k_{RearTire} = 26166 \ \frac{N}{m}$$

6.3 Suspension deflection evaluation

The stiffness values can be now used to evaluate the suspension deflections for the different loading conditions. The following equation is exploited:

$$\Delta x_{F,R} = \frac{\Delta F_{F,R}/2}{k_{F,R}} \tag{13}$$

It should be noted that the deflection values are calculated by halving the load values provided in Table 2. This adjustment is necessary because, as mentioned earlier, the previously evaluated values represent the total loads on the front and rear axles, rather than the load on an individual tire. The deflection values corresponding to the various loading conditions are presented in Table 3.

Standard	Front deflection Δx_F [mm]	Rear deflection Δx_R [mm]
A	93.8	52.8
B	99.9	61.5
C	105.9	70.2
D	107.4	83.6
E	108.9	97.0
F	110.4	110.4

Table 4: Front and Rear axle suspension deflections relative to the standard loadcases

To be noticed that at full load, i.e. when the vehicle is subjected to the loading condition described by standard F, the suspension deflections between rear and front axle are equal. This means having a perfectly balanced and horizonatal vehicle, which improves stability and enhances handling.

6.4 Ground Clearance estimation

The last step to be performed before sketching the wheel arch profile is the definition of the ground clearance. This parameter is of fundamental importance in vehicle profile design, as it plays a crucial role in the vehicle's overall performance. This parameter must be designed to achieve a good compromise between aerodynamic efficiency and the vehicle ability to overcome obstacles safely. A higher ground clearance typically reduces aerodynamic efficiency, increasing drag and affecting fuel consumption. However, it allows for easier handling on uneven surfaces and unpaved roadways. On the other hand, smaller values of ground clearance can increase the risk of scraping or damaging the undercarriage when encountering obstacles, thereby reducing the vehicle's durability. Therefore, the design must ensure that the ground clearance is sufficient to prevent interference or damage while maintaining as much aerodynamic efficiency as possible.

In this study, a ground clearance values typical of B segment vehicles is considered. It is evaluated at the maximum loading conditions, i.e. by considering load standard F. As previously mentioned, for this standard, the suspension deflection values of the analyzed vehicle are equal, resulting in a uniform ground clearance along the entire length of the vehicle side profile. The chosen ground clearance value is:

$$GC = 162.7 \text{ mm}$$

6.5 Side view wheel arch profile

Once all the data needed for the side view design of the wheel arch profile are evaluated, its shape can be sketched. As done previously for the top view design, the side view one is performed considering the maximum tire diameter that the vehicle can mount, i.e. $D = 546.2$ mm. Given the longitudinal distance between the tire and the wheel arch, evaluated in Section 4.2 and 4.3, the distance between the top of the tire and the wheel arch is evaluated considering the most critical loading condition, i.e. load standard F. In this condition, a margin of 36.5 mm between the tire and the top part of the wheel arch is considered for safety considerations. The obtained wheel arch profile is reported with color blue in Figure 18.

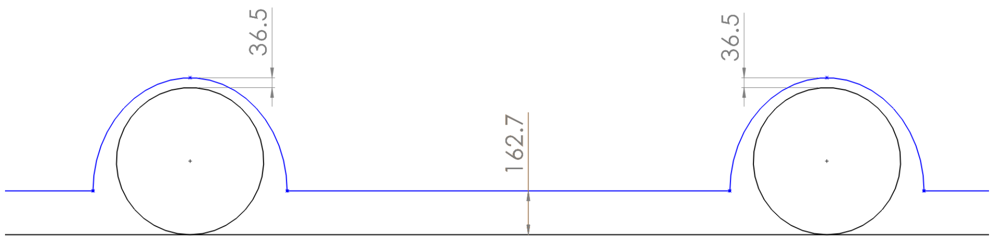

Figure 18: Wheel arch profile for loading condition of standard F

Once the wheel arch profile has been defined, it is possible to evaluate the influence of the suspensions travel, related to the loading conditions, on the ground clearance. Under loading condition A, as shown in Figure 19, due to the unequal deflection of the front and rear suspensions, the ground clearance is no longer uniform. Moreover, since the load distribution in standard A is 65% at the front and 35% at the rear, the front ground clearance is lower than the rear one. This is because the suspension deflection is greater at the front axle, indeed a lower distance between the tire and the wheel arch is present.

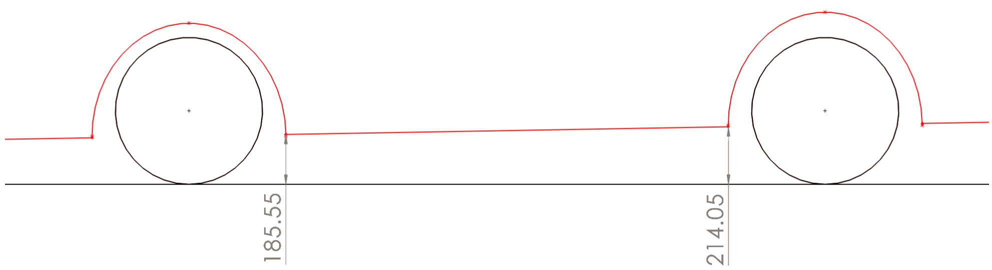

Figure 19: Wheel arch profile for loading condition of standard A

The comparison between the vehicle profile for standard A and F, corresponding to the maximum and minimum loading conditions, in depicted in Figure 20.

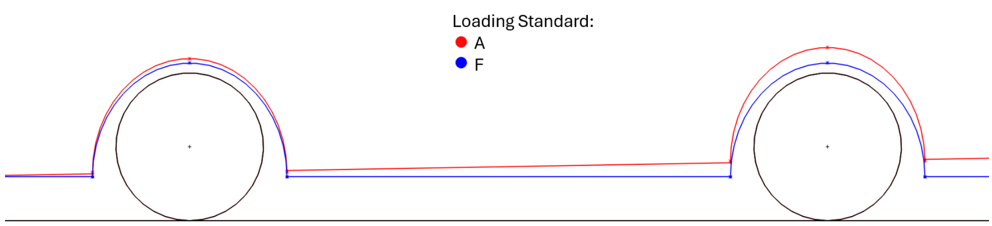

Figure 20: Wheel arch profile for loading condition of standard A and F

Once again, the ground clearance variation can be noticed through the divergence of the two undercarriage line of the vehicle's profile.

7 Conclusions

The comprehensive analysis presented in this project demonstrates the design process for the wheel arches and ground clearance of the Fiat Uno 1.0L (1989). By considering critical factors such as maximum tire size, steering angles, suspension travel, and load distribution, the study ensures the vehicle's functionality and safety under various conditions.

The integration of practical considerations such as snow chains, dirt accumulation, and suspension travel, demonstrates a thoughtful approach to real-world usability. The balance between aerodynamic efficiency and sufficient ground clearance further underscores the adaptability required in automotive design, considering both performance and practical needs.

In conclusion, this analysis serves as a benchmark for designing wheel arches and vehicle profiles. It emphasizes the importance of a complete approach, blending theoretical calculations with practical insights to create a design that meets functional and safety requirements.